Journal of Functional Materials and Applied Engineering

Review Paper

Progress on Multi-Dimensional Structural Design of Nano-Silicon Anodes for Lithium Ion Batteries

Aleksandra A. Belyonova[1], Maria Fleis[1,*]

[1] Department of Biochemistry and Food Chemistry, Lomonosov Moscow State University, 1 Leninskie Gory, Moscow 119991, Russian Federation

*Corresponding author: AABelyonova@edu.ru; Mfleis@edu.ru

Abstract. Silicon-based anode materials are considered highly promising candidates for next-generation lithium-ion battery systems, owing to their high theoretical capacity, relatively low operating potential, and abundant natural reserves. However, their practical commercialization is significantly hindered by intrinsic material limitations, including severe volumetric expansion during lithiation, poor electronic conductivity, and the formation of unstable solid electrolyte interphase (SEI) layers. These collective deficiencies result in compromised cycling durability. This review initially examines the fundamental mechanisms governing volume expansion and SEI film evolution in silicon anodes, subsequently providing comprehensive analysis of the underlying expansion phenomena. The dual failure modes (mechanical and chemical instability) were analyzed, while the detrimental consequences of cycling degradation were expounded. The modification research on silicon-based anodes in recent years was elaborated from the perspective of multi-dimensional nano-silicon structure design, including the design, preparation, advantages and disadvantages of 0D (silicon nanoparticles, silicon quantum dots, etc.), 1D (silicon nanowires and silicon nanotubes), 2D (silicon nanosheets, silicene), and 3D (porous silicon, silicon nanosponges) nano-silicon materials, as well as the differences in structure, performance and application of other silicon-based anode materials (pure Si anode, SiO_x anodes, Si/C composite anodes). Finally, the critical requirements for advancing novel technological innovation, deepening mechanistic fundamental insights, developing in-situ characterization techniques, and implementing synergistic modification strategies were emphasized. Future research directions and application prospects for high-performance silicon-based anode materials were subsequently outlined.

Keywords: *lithium-ion batteries (LIBs); silicon-based anodes; nano-structure; material modification strategies; structural control*

Received on 10 Apr 2022, Accepted on 15 June 2022, Published on 08 July 2022

1 Introduction

In recent years, the sustained escalation of worldwide energy consumption has catalyzed advancements in sustainable technologies and electrochemical storage systems. Lithium-ion batteries, distinguished by their elevated energy density, extended operational lifespan, and compact form factor, have emerged as the predominant solution for rechargeable energy storage across portable electronics, electric mobility platforms, and grid-scale infrastructure. Currently, the global LIBs market value is USD 48 billion, and it is expected to increase to USD 182.53 billion by 2030 [1]. However, the energy density of LIBs currently on the market is mediocre, failing to meet the rapidly growing demand for driving range of electric and hybrid vehicles. Consequently, accelerating the advancement of high-energy-density lithium-ion battery technology holds paramount importance.

The core components of LIBs include cathode, anode, electrolyte and separator. Among them, the anode and cathode active materials undertake the function of energy storage. Silicon-based anode materials deliver an exceptionally high theoretical specific capacity of 4200 mA·h/g, coupled with abundant natural reserves, favorable cost profiles, and benign environmental impact. A lithiation potential near 0.4 V not only raises the overall operating voltage of the full cell but also effectively suppresses lithium dendrite formation [2]. Leveraging

these advantageous characteristics, silicon has gained broad recognition as one of the most attractive negative electrode candidates for lithium-ion batteries and has become a focal point of current research endeavors.Nevertheless, the intrinsically limited electronic conductivity of silicon (1×10^{-5}–1×10^{-3} S/cm) and sluggish lithium ion diffusion kinetics (1×10^{-14}–1×10^{-13} cm^2/s) render silicon anodes susceptible to severe volumetric expansion (300%–400%) during lithiation [3], imposing substantial mechanical stress on active material particles and inducing surface fracture, fragmentation, and pulverization. Furthermore, during initial charge-discharge cycling, electrolyte decomposition at the silicon particle surface generates a solid electrolyte interphase film. The recurring volumetric breathing of silicon particles during subsequent cycling causes repeated SEI rupture and regeneration, progressively degrading and thickening this passivation layer [4–5]. The combination of poor mechanical integrity in silicon particles and SEI film instability ultimately compromises electrochemical reversibility and accelerates capacity degradation, constraining commercial viability [6–8]. To date, multiple methods have been adopted to address these challenges, including nanomaterial design, morphology control, carbon coating and matching appropriate electrolyte systems [9-14]. Among them, nanostructure design is a very effective method, which can shorten Li^+ transport distance and reduce polarization. Moreover, nanoscale silicon, by virtue of its increased specific surface area and strengthened interatomic binding energy, not only enlarges the electrolyte interfacial contact region, enhances the utilization efficiency of active lithium ions, and expedites the kinetics of alloying reactions, but also enables efficient stress relaxation within silicon particles during volume expansion, thereby alleviating mechanical deformation and consequently reducing the likelihood of particle pulverization while maintaining acceptable cycling stability [15–16].

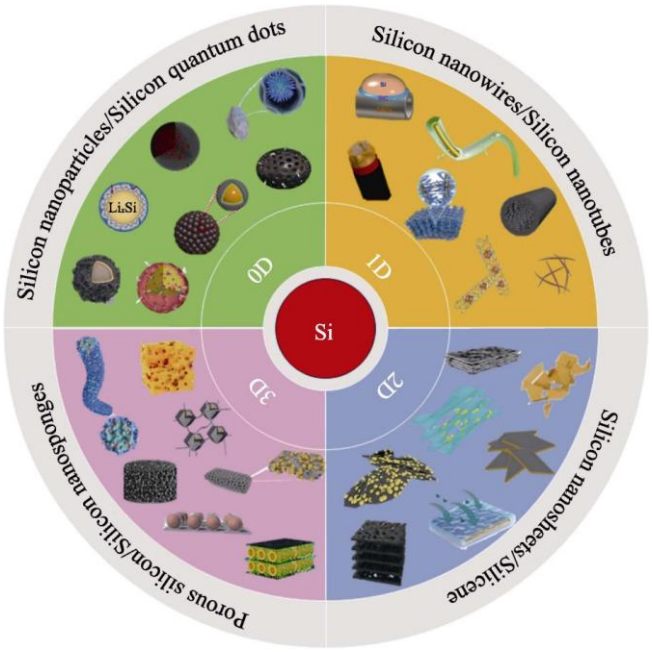

Figure 1 Schematic diagram of nanostructures for silicon-based anode materials

The present investigation adopts the failure mechanism of silicon-based anode materials as its foundational analytical framework. It first introduces the fundamental principles underlying volumetric expansion and solid electrolyte interphase (SEI) film evolution in silicon-based negative electrodes, followed by a thorough investigation of the expansion mechanisms involved and a critical evaluation of the resulting cycling instability. Then, the modification research on Si-based anodes in recent years is elaborated from the perspective of multi-dimensional nano-Si structure design (Fig. 1). Finally, prospective trajectories for the future evolution and practical deployment of silicon-based negative electrode materials are outlined.

2 Failure Mechanisms of Silicon-Based Anode Materials

Despite silicon's exceptionally high theoretical specific capacity, its intrinsic material characteristics render silicon-based anode formulations highly unstable during electrochemical cycling, manifesting as rapid capacity

attenuation [17-20]. With progressive advancements in microscopic imaging modalities and surface-sensitive quantitative analytical techniques, the structural and chemical evolution occurring within silicon-based anodes throughout cycling has been systematically investigated [21-23]. Contemporary studies demonstrate that the degradation mechanisms of silicon-based anode materials can be systematically classified into two primary categories: mechanical instability and chemical instability.

2.1 Mechanical Instability

2.1.1 Conversion Reaction

Capacity degradation in silicon anodes stemming from mechanical instability can be ascribed to fracture initiation driven by anisotropic lithium insertion and the substantial volumetric expansion accompanying lithiation and delithiation processes [24]. As an anode material, Si involves alloying reactions with lithium in the lithium storage mechanism, as shown in Eqs. (1)~(4):

Si+xLi++xe−→LixSi(1)

LixSi+(3.75−x)Li++(3.75−x)e−→Li15Si4(2)

Li15Si4→LixSi+yLi++ye−+Li15Si4(3)

LixSi→Si+xLi++xe−(4)

Eqs. (1) and (2) represent the initial lithiation process, where Li^+ combines with crystalline Si to form amorphous Li_xSi ($0 \le x \le 4.4$), with a large number of Li surrounding Si [25]. When the potential drops to ~50 mV, the amorphous Li_xSi further transforms into the amorphous $Li_{15}Si_4$ (a-$Li_{15}Si_4$) phase. This lithiated phase with elevated lithium content enables silicon materials to attain a theoretical specific capacity of 3580 mA·h/g under ambient conditions. Significantly, during initial lithiation, crystalline silicon undergoes transformation to an amorphous state, with all subsequent reactions proceeding within this amorphous matrix. Throughout this process, fracture of crystalline silicon generates Si–Si single bonds and isolated silicon atoms, which are progressively integrated into amorphous $Li_{15}Si_4$ as fragmented structural units, progressively dismantling the original crystalline architecture [26]. Each silicon atom can potentially accommodate up to 4.4 lithium atoms, yielding $Li_{4.4}Si$ as the terminal lithiation product. Notably, silicon crystallizes in a unit cell with volume of 0.04088 nm^3, whereas the fully lithiated $Li_{4.4}Si$ phase exhibits a substantially expanded unit cell volume of 0.1617 nm^3. This pronounced disparity confirms that silicon undergoes severe volumetric expansion of 300%–400% [27]. The ultimate lithiation product $Li_{3.5}Si$ is characterized by approximately 280% volume expansion. Although marginally less extreme than $Li_{4.4}Si$, this expansion substantially exceeds that of LiC_6 [28]. In contrast, graphite anodes provide six carbon host sites per lithium ion; this structural distinction engenders severe volumetric expansion in silicon-based anodes during lithium insertion and extraction, readily inducing particle fracture and pulverization, subsequent electrode structural collapse, and eventual detachment of active material from the current collector [29].

During the delithiation process, as shown in Eqs. (3) and (4), when the potential rises to ~0.4 V, the $Li_{15}Si_4$ phase reversibly transforms back into a-Si, accompanied by significant volume shrinkage. At this time, the fracture of conductive paths inside the active material and the inability of residual $Li_{15}Si_4$ phase to be fully delithiated jointly lead to increased irreversible capacity, significantly reducing the initial Coulombic efficiency (CE).

The alloying reaction between silicon and lithium exhibits substantial temperature-dependent variation [30]. At high temperatures (450 °C), the lithiation of silicon proceeds in a stepwise manner, driven by enhanced molecular mobility and accelerated reaction kinetics. This process is accompanied by the successive emergence of four thermodynamically stable crystalline phases: $Li_{12}Si_7$ (0.332 V), $Li_{14}Si_{16}$ (0.288 V), $Li_{13}Si_4$ (0.157 V), and $Li_{22}Si_5$ (0.044 V). Notably, the $Li_{22}Si_5$ phase enables Si anodes to reach their highest theoretical specific capacity (4200 mA·h/g) at high temperatures. At room temperature, lithiation/delithiation shows continuous decreasing and increasing trends [29,31-32] (Fig. 2).

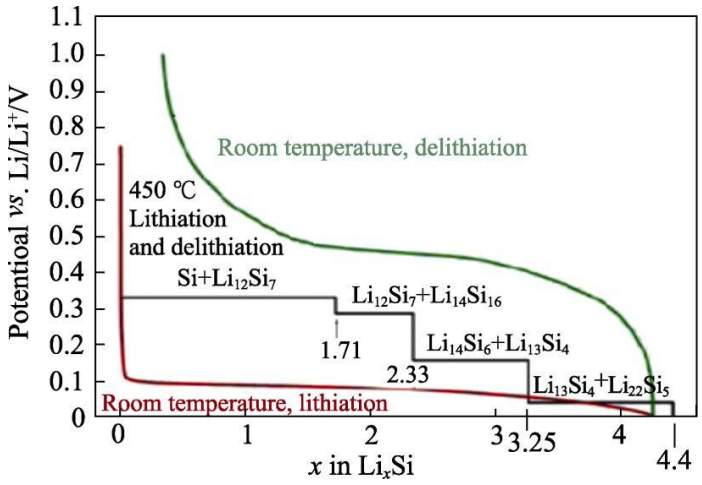

Figure 2 Electrochemical alloying curves of Si and Li at room temperature and high temperature (under ideal conditions) [29]

2.1.2 Anisotropic Lithiation

The lithiation process of silicon proceeds through two sequential stages. In the initial stage, lithium undergoes sustained diffusion within a core–shell architecture, wherein the characteristic diffusion timescale (τ_D) describes the transport behavior of lithium atoms across the lithiated silicon shell (Li_xSi). The second stage comprises phase transformation reactions occurring at the two-phase boundary, with the reaction characteristic timescale (τ_R) describing the intrinsic chemical reaction and phase transition kinetics at this interface. For nanoscale silicon, τ_D is generally considerably smaller than τ_R, which implies that the propagation of the two-phase interface is significantly slower than lithium diffusion. Consequently, the silicon-to-alloy conversion rate at the interface constitutes the rate-determining step governing the overall lithiation process [33–34]. Given that silicon lithiation operates through a two-phase reaction mechanism, bond cleavage and atomic reorganization are essential for the reaction to proceed. Consequently, fracture predominantly initiates between adjacent {110} crystallographic planes along the nanopillar sidewalls. In contrast to crystalline silicon, amorphous silicon undergoes isotropic expansion without preferential crack propagation, exhibiting superior structural stability—for instance, lower compressive stress during lithiation relative to crystalline silicon (Fig. 3c) [38–39].

2.2 Chemical Instability

The chemical instability of silicon-based anodes is predominantly governed by the recurrent fracture and reconstruction of the solid electrolyte interphase (SEI) layer, which serves as the foremost degradation mechanism [40–41]. Throughout charge-discharge cycling, the SEI film morphology on silicon anode surfaces undergoes continuous evolution concomitant with particle volumetric fluctuations. During anode expansion and contraction, the SEI film on silicon surfaces becomes susceptible to fracture, thereby exposing fresh, unreacted silicon surface to the electrolyte environment. In the subsequent reaction process, additional SEI film continues to form on the Si surface (Fig. 4) [42], further consuming a large amount of Li and electrolyte, ultimately leading to a decrease in irreversible capacity and greatly shortening its cycle life [43-45]. Furthermore, the SEI film exhibits a bilayer architecture, with tensile stresses generated during cycling inducing fracture within the outer SEI stratum [46-47]. Progressive temporal evolution leads to delamination at the inner-outer layer interface, ultimately culminating in SEI film detachment. Additionally, SEI formation is not restricted to particle exterior surfaces but can also occur intraparticularly, engendering irreversible volumetric expansion. Through iterative repetition of this process, the SEI film progressively thickens, thereby driving irreversible volume expansion and diminished Coulombic efficiency. Throughout this evolution, the thickened, electronically insulating SEI film impedes both lithium ion and electron transport, resulting in elevated interfacial impedance and substantial degradation of cycling stability and rate capability in silicon anodes. In addition, during battery storage, the SEI film is in a dynamic dissolution-regeneration cycle, with a general trend of thickening, leading to increasing aging of materials through the consumption of active ions and increased impedance [48].

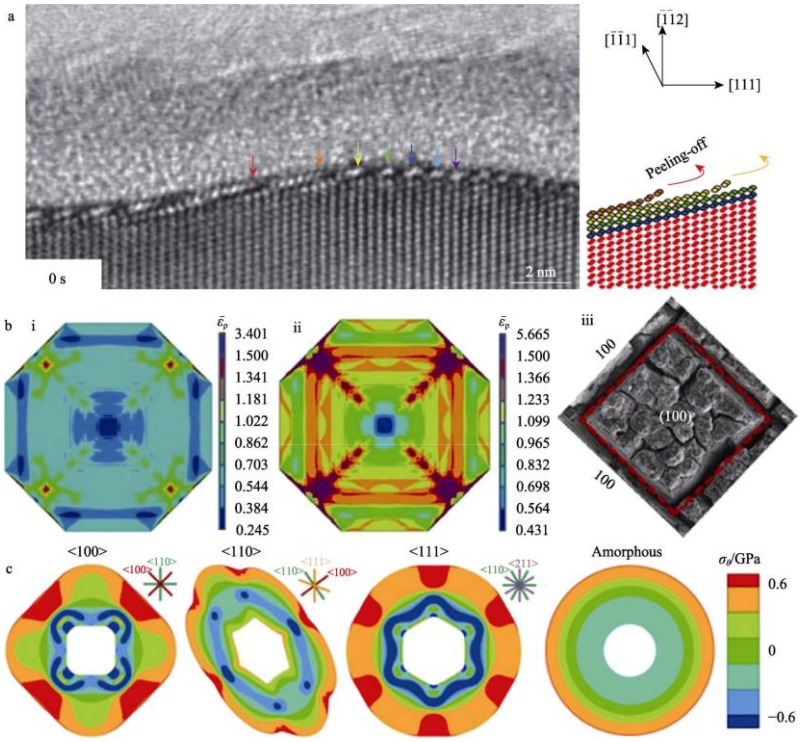

Figure 3 Ledge mechanism of crystalline silicon (a) [35]; Finite element results of lithiated (i) and delithiated (ii) Si electrode and SEM image (iii) of crack formation in <100> directions (b) [37]; Finite element simulation of stress evolution of <100>, <110>, <111>, and a-Si nanotubes (c) [38-39]

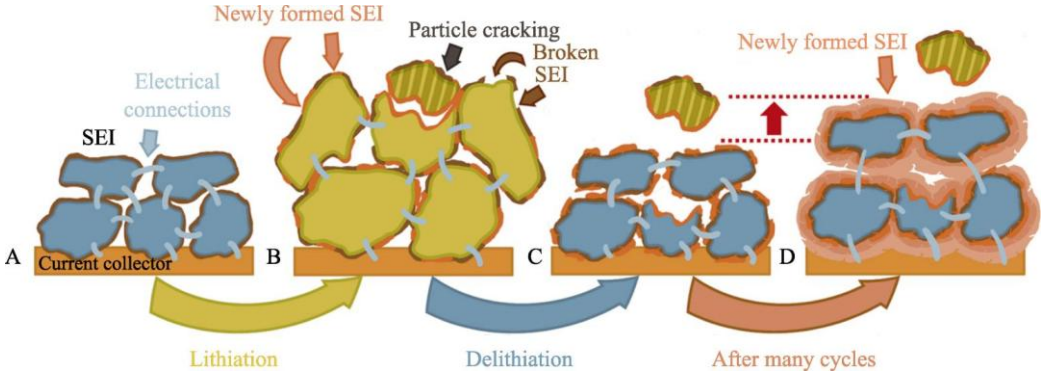

Figure 4 Schematic diagram of degradation mechanism of SEI-driven silicon-based anode [42]

Based on the preceding failure mechanism analysis of silicon-based anode materials, it is evident that the alloying reaction occurring during lithium storage induces substantial volumetric expansion in silicon-based materials, leading to cyclic SEI film reformation and progressive electronic insulation. This extensive irreversible lithium consumption and accumulation of electrochemically inactive lithium significantly compromise the cycling stability of lithium-ion batteries (Fig. 5). During initial cycling, rapid capacity fade is predominantly attributable to lithium depletion within silicon-based anodes, driven by continuous SEI formation, growth, and structural reorganization; in subsequent cycles, capacity degradation proceeds more gradually due to surface fracture of the silicon anode material; prolonged cycling instability is principally caused by active material pulverization and detachment from the electrode architecture [49].

3 Nanostructure Design

Nanoscale architecture engineering constitutes a critical strategy for improving the structural integrity of silicon-based negative electrodes. Through rational nanostructure engineering of silicon materials, efficient stress

relaxation can be achieved, which substantially improves fracture resistance and thereby effectively suppresses mechanical damage induced by lithiation-induced stress. Its advantages include shortening the diffusion path of Li^+ and reducing electrode polarization; increasing the specific surface area of materials to enhance contact with electrolyte, improving the utilization rate of active lithium and the kinetics of alloying reactions; surface atoms with elevated binding energy can effectively accommodate volumetric expansion stress and suppress structural degradation [50]. The evolution of silicon nanostructuring from zero-dimensional nanoparticles through one-dimensional nanowires and nanotubes, extending to two-dimensional nanosheets, and culminating in three-dimensional porous architectures provides an essential design framework for simultaneously controlling volumetric expansion and enhancing electronic conductivity (Fig. 6) [51].

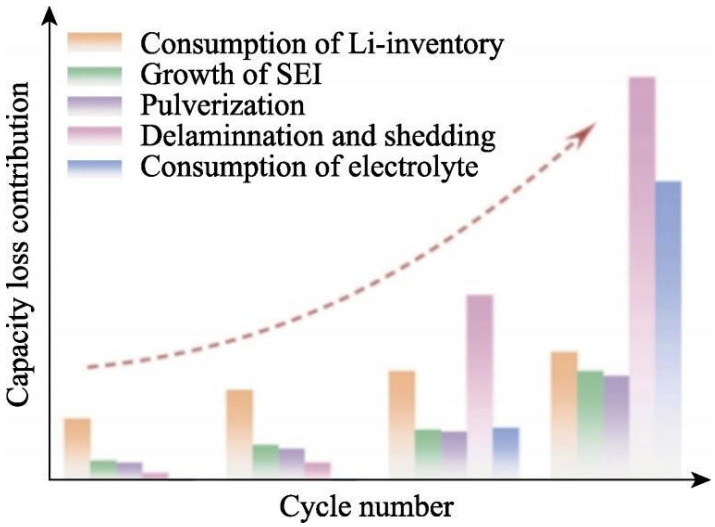

Figure 5 Schematic diagram of probable failure mechanism of Si-based anodes during battery charging and discharging [49]

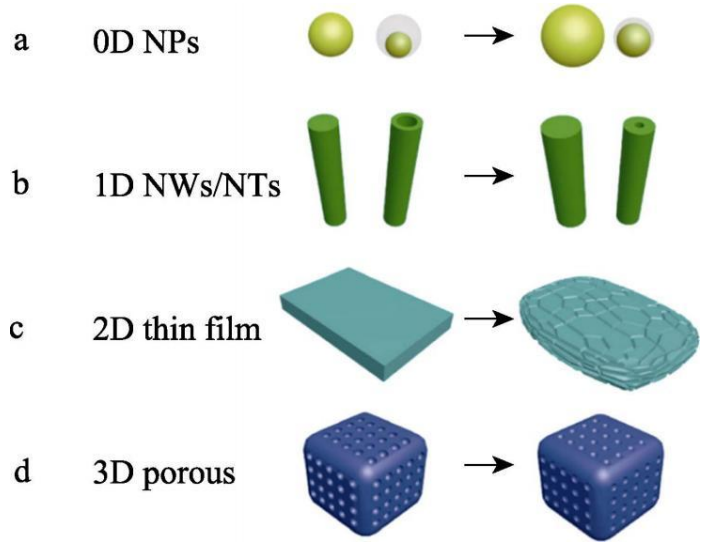

Figure 6 Schematic diagram of Si nanostructure and morphology change after cycling [51]

In recent years, numerous fabrication and modification methodologies for nanostructured silicon-based anodes have been developed, encompassing metal-assisted chemical etching, chemical vapor deposition, sol-gel synthesis, templating approaches, mechanical ball milling, and spray drying techniques [52]. Modification of synthesis protocols and processing conditions for nanostructured silicon-based anode materials enables effective regulation of structural parameters including pore dimensions, particle size, and specific surface area. Table 1 summarizes the electrochemical performance characteristics of representative nanostructured silicon-based

anode materials.

Table 1 Performance comparison of nano-silicon anode materials by structural architecture

Structure	Material name	Preparation method	Cycling performance / (mA·h/g)	Cycle number / cycles	Mass current density / (A/g)	Capacity retention rate / %	Ref
0D	Si-CBPOD	In-situ polymerization + carbonization	1110.8	1000	4	75.6	[53]
	MPCF@VG@SiNDs/C	Dual-template method + sol-gel method	1301.4	1000	1	—	[54]
1D	Si@SiOx@BNCNT	In-situ pyrolysis	1700.0	700	0.2	—	[55]
	SiNW/CNF/CNT	MACE	1602.0	1000	—	56.0	[56]
2D	pSi@C	Sol-gel method + magnesiothermic reduction + thermal decomposition	2236.0	150	1	71.5	[57]
	Si-NSs@C/NG	Ball milling + catalytic pyrolysis	807.9	120	0.2	81.0	[58]
3D	Si@PVPC	Sol-gel method + carbonization + acid washing	1294.3	1400	2	85.5	[59]
	VGs@Si@PCFs	Electrospinning + magnetron sputtering + CVD	2205.0	3000	1	83.5	[60]

Note: "—" indicates not mentioned in the reference, the same below.

The metal-assisted chemical etching approach primarily employs noble metals—including gold, silver, and platinum—as catalytic agents to selectively corrode silicon wafers within a mixed solution containing hydrofluoric acid and oxidizing species such as hydrogen peroxide, ferric nitrate, and permanganate. The process is relatively simple and low-cost, and can customize Si nanostructures with different morphologies and sizes. However, it uses hazardous chemicals such as HF, noble metal catalysts are difficult to recover, and the synthesized material structure has poor uniformity. The CVD method deposits materials on the substrate surface via gas-phase reactions to endow materials with new properties, such as depositing carbon on the Si surface. Its advantages include ultra-high specific capacity and cycling stability of prepared materials, precise and controllable structure design, and high material purity and consistency. However, the preparation process control is complex, carbon layer uniformity and adhesion are insufficient, and equipment and material costs are high. The template method mainly uses substrates with specific structures and shapes as templates, and removes the templates via chemical corrosion or high-temperature pyrolysis to obtain the required nanostructures, such as porous structures. Its advantages include precise and controllable material structure, low requirements for process equipment, and low cost. However, mass production is difficult, and the prepared material structure has poor stability. The mechanical ball milling method uses the rotation and vibration of balls to violently impact and grind raw

materials, crushing large particle powders into NPs. The process has high maturity, low equipment investment, and high flexibility in composite structure, but the degree of nanostructuring is limited, agglomeration is serious, and impurities are easily introduced.

3.1 0D Si-Based Anode Materials

The electrochemical characteristics of silicon-based negative electrodes can be further enhanced through the introduction of non-metallic dopants into zero-dimensional architectures [61–62]. YU et al. [53] synthesized a porous carbonaceous coating co-doped with nitrogen and sulfur to homogeneously encapsulate silicon particles, thereby forming a multifunctional protective shield. This novel structural design effectively stabilized the interfacial region between the electrode and electrolyte while alleviating volumetric expansion of silicon. The N–S co-doped framework markedly elevated both electronic and ionic transport capabilities. Furthermore, the carbonization treatment increased the elastic modulus of the protective layer and reorganized the silicon–carbon boundary, promoting the formation of robust covalent bonds [63]. The resulting composite achieved a reversible specific capacity of 1110.8 mA·h/g after 1000 cycles at 4 A/g, together with an energy density of 574 W·h/kg and capacity retention of 75.6% following 300 cycles at 0.2C.

WANG et al. [64] fabricated a core-shell heterostructure (Si@V_3O_4@C) through a facile solvothermal protocol, comprising a silicon core encapsulated by a V_3O_4@C shell. Computational modeling demonstrated that the in-situ formed vanadium oxide layer promotes rapid lithium ion diffusion and lowers the activation energy for lithium transport from the carbon shell to the silicon core. The three-dimensional amorphous carbon architecture considerably boosts electronic transport and mechanical stability. After systematic optimization, the Si@V_3O_4@C electrode displayed remarkable cycling endurance at 0.5 A/g, achieving a reversible specific capacity of 1061.1 mA·h/g following 700 cycles, alongside 70.0% capacity retention and an average Coulombic efficiency of 99.3%.

HU et al. [65] utilized a classic heat treatment process to innovatively design and construct a high-mechanical pure Si anode with defect (stacking faults, nanotwins and moiré crystals) continuously pinned and strengthened nanograins based on crystalline silicon industry waste. It exhibited far superior stability compared to traditional crystalline or amorphous Si materials. After repeated lithiation/delithiation, these strengthened grains still firmly rooted in the Si substrate without amorphization, thereby driving the optimization of the external protective SEI film and stabilizing the electrode. Comprehensive molecular dynamics simulations clarified the grain generation and strengthening mechanisms. The optimized silicon electrode, prepared with an active material mass loading of 80%, achieved a reversible specific capacity of 2180.9 mA·h/g after 200 cycles at a specific current of 0.8 A/g.

The combination of 0D Si structure design with carbon materials has been a research hotspot in recent years. SHIN et al. [66] prepared SiC composites via a "one-pot" hydrothermal technique, using etched and modified SiNPs and sucrose as carbon precursors. The as-prepared SiC composites feature a meso-macroporous architecture, in which a considerable loading of silicon nanoparticles (40 wt%) is encapsulated within 3 μm carbon spheres. This composite material exhibits an elevated initial specific capacity of 1300 mA·h/g, maintains 90% capacity retention over 200 cycles, and enables rapid charge–discharge cycling accomplished in 12 minutes.

LI et al. [54] employed a dual-templating approach integrated with sol-gel methodology to uniformly distribute amorphous silicon nanodots within carbon nanospheres, subsequently anchoring these composites onto macroporous carbon framework walls via vertical graphene interconnects to fabricate a distinctive MPCF@VG@SiNDs/C architecture (Fig. 7). The ultrafine silicon nanodots (particle size ~0.7 nm) exhibit exceptional dispersibility and amorphous structural characteristics. Vertical graphene furnishes flexible, directional electron and lithium ion transport pathways, while the macroporous carbon framework provides abundant lithium storage sites and rapid lithium ion diffusion channels. The half-cell, manufactured in accordance with industrial electrode specifications, exhibited superior cycling durability (reversible specific capacity of 1301.4 mA·h/g after 1000 cycles at 1 A/g without significant degradation) and remarkable rate performance (910.3 mA·h/g at 20 A/g). The assembled pouch full cell attained high energy density (1694.0 W·h/L, 602.8 W·h/kg) and exceptional fast-charging capability (498.5 W·h/kg, with 3C charging accomplished in 16.8 minutes).

In conclusion, the development of zero-dimensional silicon nanoparticles marks a substantial advancement in improving the electrochemical performance of lithium-ion batteries. The architectural design integrating silicon nanoparticles with porous and hollow configurations demonstrates exceptional electrochemical characteristics, attributable primarily to the following factors: First, internal voids and porosity accommodate the volumetric expansion of silicon-based anode materials, effectively mitigating dimensional fluctuations during charge-discharge cycling. This distinctive attribute preserves material structural integrity, enabling repeated cycling without substantial performance deterioration. Additionally, the porous structural configuration shortens the transport distances for both electrons and lithium ions, which effectively alleviates polarization phenomena [67]. By reducing the distance that Li^+ and electrons need to travel, materials can be charged and discharged quickly, making them ideal for high-performance battery applications. In addition, the SiNPs structure reduces the local current density, thereby reducing the stress gradient near the particle surface, and these nanostructures enable the material surface to have a more uniform distribution of electrochemical reactions, maintaining their performance during multiple cycles. However, the disadvantages of SiNPs are also prominent, such as easy agglomeration, leading to uneven contact between active materials and electrolyte, and rapid capacity fading; easy structural pulverization, particle crushing after repeated expansion/contraction, damaging the electrode structure, and low cycle life (usually <100 cycles); poor material conductivity, requiring combination with conductive agents (such as carbon), otherwise the charge transport efficiency is low.

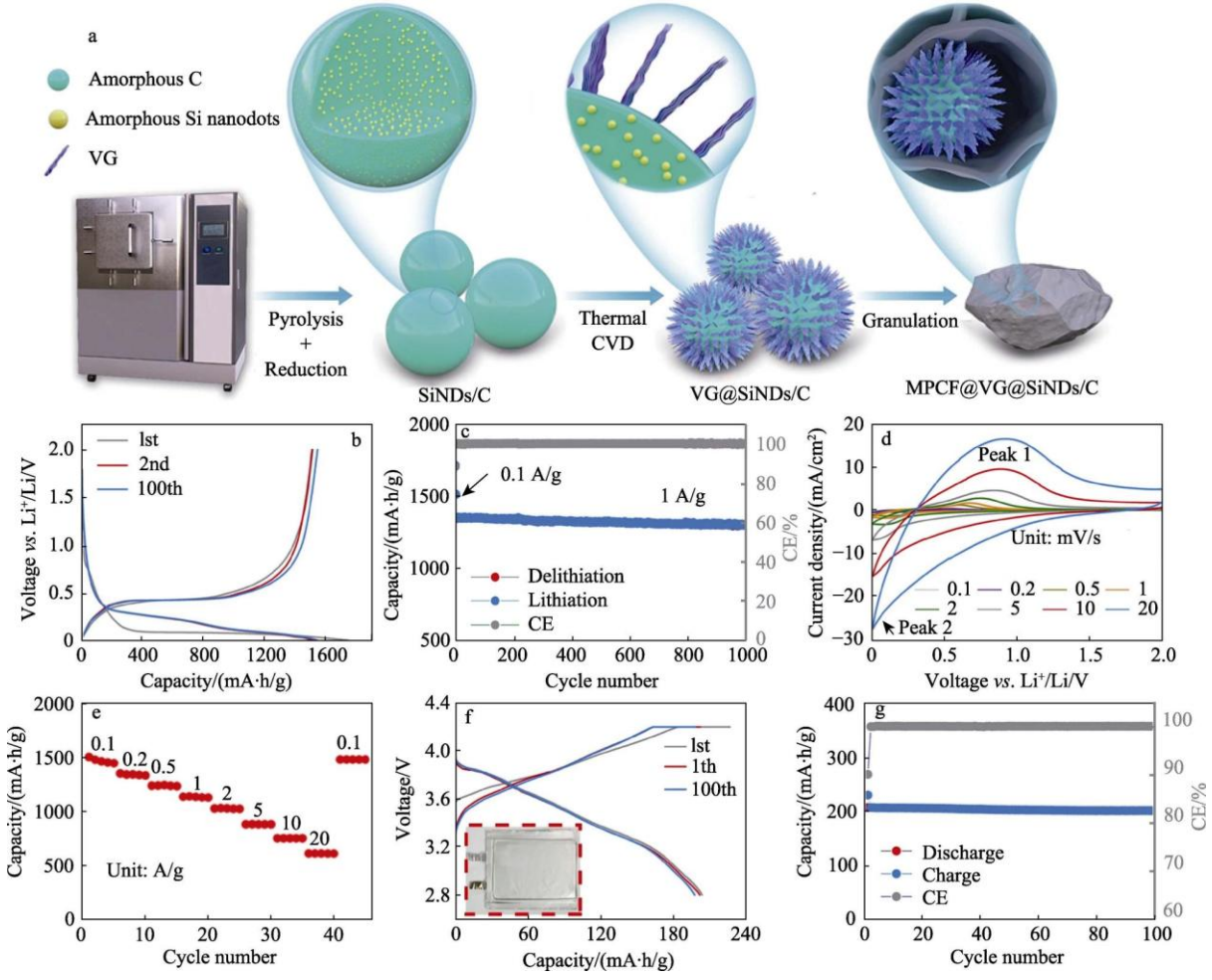

Figure 7 Schematic diagram of synthesis process of MPCF@VG@SiNDs/C [54]

3.2 1D Si-Based Anode Materials

Representative materials of 1D Si nanostructures include SiNWs and SiNTs, which have the following unique properties: First, 1D Si nanomaterials can alleviate mechanical strain during radial volume changes of materials,

preventing material pulverization. Second, 1D structures promote effective electron transfer inside and on the surface of materials, ensuring rapid charge transfer, thereby improving electrochemical performance. Benefiting from the structural advantages of 1D Si-based anode materials, they show good adaptability in coping with internal stress of electrodes, and also help the contact between conductive agents, active substances and current collectors, showing good electrical conductivity. The main preparation methods of 1D SiNWs/SiNTs include template method, CVD, MACE, molecular beam epitaxy, laser ablation and liquid-phase preparation methods [68].

The template method is currently the simplest method to prepare 1D Si-based nanostructures, with low requirements for the experimental environment. ZHAO et al. [69] harnessed a Si–Mg alloy scaffold together with a polydopamine precursor to construct a one-dimensional tubular silicon/nitrogen-doped carbon hybrid (Si@NC). Microstructural characterization via scanning electron microscopy confirmed that the silicon domains possessed approximate dimensions of 100 nm. The resulting Si@NC material delivered outstanding specific capacity, favorable redox reaction kinetics, and excellent cycling stability, attaining a reversible specific capacity of 583.6 mA·h/g following 200 cycles at a current density of 0.5 A/g. The hollow tubular configuration and the confinement of silicon within the nitrogen-doped carbon matrix cooperatively buffered volume expansion, thereby endowing the lithium-ion battery system with markedly enhanced cycling durability. CHEN et al. [70] used cellulose nanocrystals (CNC) as a template, utilizing their surface chemical properties and unique self-assembly behavior to create a CNC network template, and processed it to design Si materials for energy storage applications, called Si nano-quills (SiNQ). The SiNQ structure has a porous tubular morphology, which not only has a strong ability to store Li^+, but also maintains its structural integrity. The presence of low-oxidation-state silicon within the silicon nanostructure is critical for attaining stable cycling performance in lithium-ion batteries. Surface Si–H bonds confer aqueous dispersibility, facilitating fabrication of water-based silicon-graphite electrodes with favorable environmental and economic implications. In silicon nanostructure-graphite composites, incorporation of merely 17 wt% silicon nanostructures elevates graphite anode capacity by approximately 2.5-fold. Combined with multifunctional pre-lithiation strategies, the initial Coulombic efficiency of lithium-ion batteries can reach 97.5%. The high active-loading silicon nanostructure-graphite anode demonstrated exceptional cycling stability over 500 cycles, maintaining an average Coulombic efficiency exceeding 99% under charge-discharge conditions at 5.4 mA/cm² current density.

Compared with the template method and MACE method, the CVD method has a fast growth rate and is suitable for large-scale preparation. DI et al. [71] successfully fabricated a sandwich-structured anode architecture (CNT/SiNPs/SiC) via chemical vapor deposition coupled with magnesiothermic reduction, wherein silicon nanoparticles are interposed between carbon nanotubes and silicon carbide layers. The silicon carbide stratum functions as a rigid mechanical constraint to suppress silicon volumetric stress, while the internal graphitic carbon nanotube network serves dual roles as a stress-buffering matrix and electron conductive pathway. Furthermore, the silicon carbide-carbon nanotube combination alleviates surface stress at the carbonaceous interface, synergistically preventing integrated structural degradation and SEI film reorganization. Additionally, the SiC (111) crystallographic plane exhibits strong adsorption affinity for fluoroethylene carbonate molecules, contributing to enhanced SEI film stability. Consequently, the CNT/SiNPs/SiC anode delivered a specific capacity of 1127.2 mA·h/g at 0.5 A/g, with 95.6% capacity retention after 200 cycles, and exceptional rate performance of 745.5 mA·h/g at 4.0 A/g, maintaining 85.5% capacity retention after 1000 cycles.

In summary, the advancement of one-dimensional silicon-based anode materials represents a transformative development in lithium-ion battery negative electrode technology. The structural attributes of silicon nanowires and nanotubes effectively mitigate volumetric expansion of the active material while facilitating faster electron transfer kinetics, thus contributing to improved overall battery performance. At the nanoscale, one-dimensional silicon anodes fundamentally alter the dynamics governing lithium ion intercalation and deintercalation processes. However, the preparation cost of 1D Si nanomaterials is high, requiring CVD or template methods, with complex processes and difficulty in scaling up; second, their tap density is low, and the gaps between nanowires are large, leading to low volumetric energy density of electrodes, limiting practical applications; in addition, their surface side reactions are numerous, and the large specific surface area easily reacts with electrolyte, forming a thick SEI film and consuming Li^+. Currently, diverse innovative fabrication methodologies including chemical etching, self-assembly, and chemical vapor deposition [68] have been successfully employed to synthesize one-dimensional silicon nanostructures with advantageous characteristics such as volumetric

expansion mitigation and enhanced electrochemical properties. These developments have spurred the progression of silicon nanostructures integrating multifunctional architectural features, including mesoporous channels, carbon-based protective coatings, and yolk–shell geometries. Such structural optimizations effectively alleviate critical challenges, notably volumetric expansion and mechanical degradation, encountered by silicon-based anodes during electrochemical cycling in lithium-ion systems. Chemical vapor deposition and metal-assisted chemical etching techniques have proven effective as scalable approaches for fabricating highly ordered silicon nanowires and nanotubes with accurately tunable dimensions and desirable electrochemical properties. The evolution of one-dimensional architectures, exemplified by mesoporous silicon nanowire arrays and silicon nanostructure nanotubes, enables silicon-based anodes to alleviate detrimental volumetric expansion effects while maintaining elevated specific capacity. Moreover, the integration of carbon coatings with flexible substrates has emerged as a practical strategy for enhancing structural integrity and improving electronic conductivity in silicon-based anode materials—a crucial factor for sustaining long-term cycling stability in lithium-ion batteries. Notably, the efficacy of these nano-engineered one-dimensional silicon anode architectures extends cell cycle life while substantially elevating specific capacity.

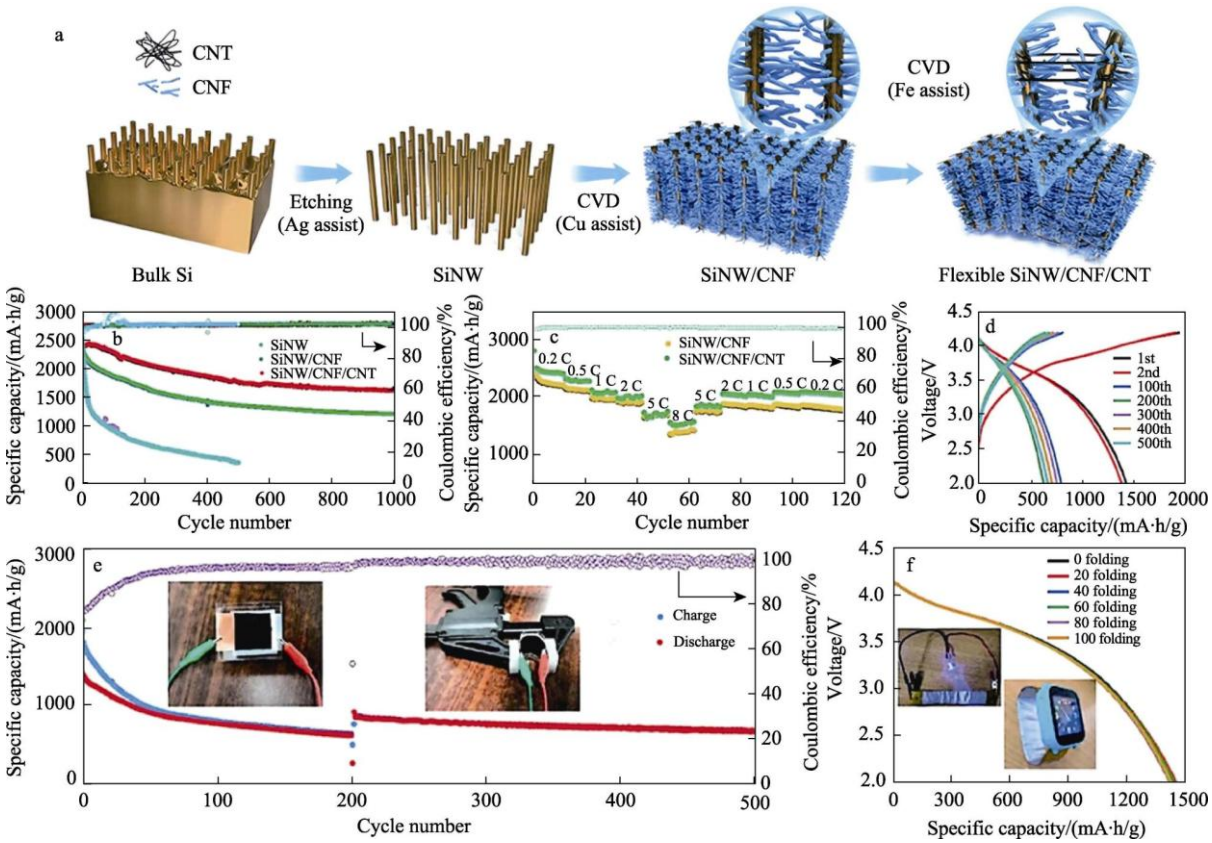

Figure 8 Schematic diagram of synthesis process of SiNW/CNF/CNT array

3.3 2D Si-based Anode Materials

Two-dimensional (2D) silicon nanomaterials, encompassing silicon nanosheets (Si-NSs) and the theoretically compelling allotrope silicene, represent a decisive architectural evolution in the pursuit of high-energy-density lithium-ion batteries (LIBs). Defined by an ultra-thin layered morphology with thicknesses rigorously constrained below 10 nm, these materials exploit low-dimensionality to resolve the intrinsic mechanical and kinetic limitations of bulk silicon anodes. The defining advantage of the 2D geometry lies in its extreme aspect ratio: lateral dimensions extend across micrometric scales, while vertical confinement reduces diffusion pathways to just a few atomic layers. This morphology fundamentally reshapes lithium-ion transport dynamics. In conventional bulk silicon, Li^+ diffusion is hindered by long, tortuous pathways that induce concentration polarization and mechanical fracture. In contrast, 2D Si-NSs truncate the vertical diffusion distance to

near-atomic scales, allowing Li^+ to traverse the active material within seconds even at high current densities. Simultaneously, the planar basal plane facilitates rapid lateral ion transport, effectively decoupling ionic flux from volumetric strain. The ultra-thin structure also confers exceptional mechanical flexibility, enabling elastic accommodation of the 300–400% volume expansion associated with full lithiation without catastrophic pulverization. Furthermore, the high specific surface area maximizes the density of electrochemically active sites, enhancing Li^+ adsorption and deintercalation kinetics. This architectural paradigm shifts the failure mode of silicon anodes from brittle fracture to reversible elastic deformation, positioning 2D silicon as a transformative platform for next-generation energy storage.

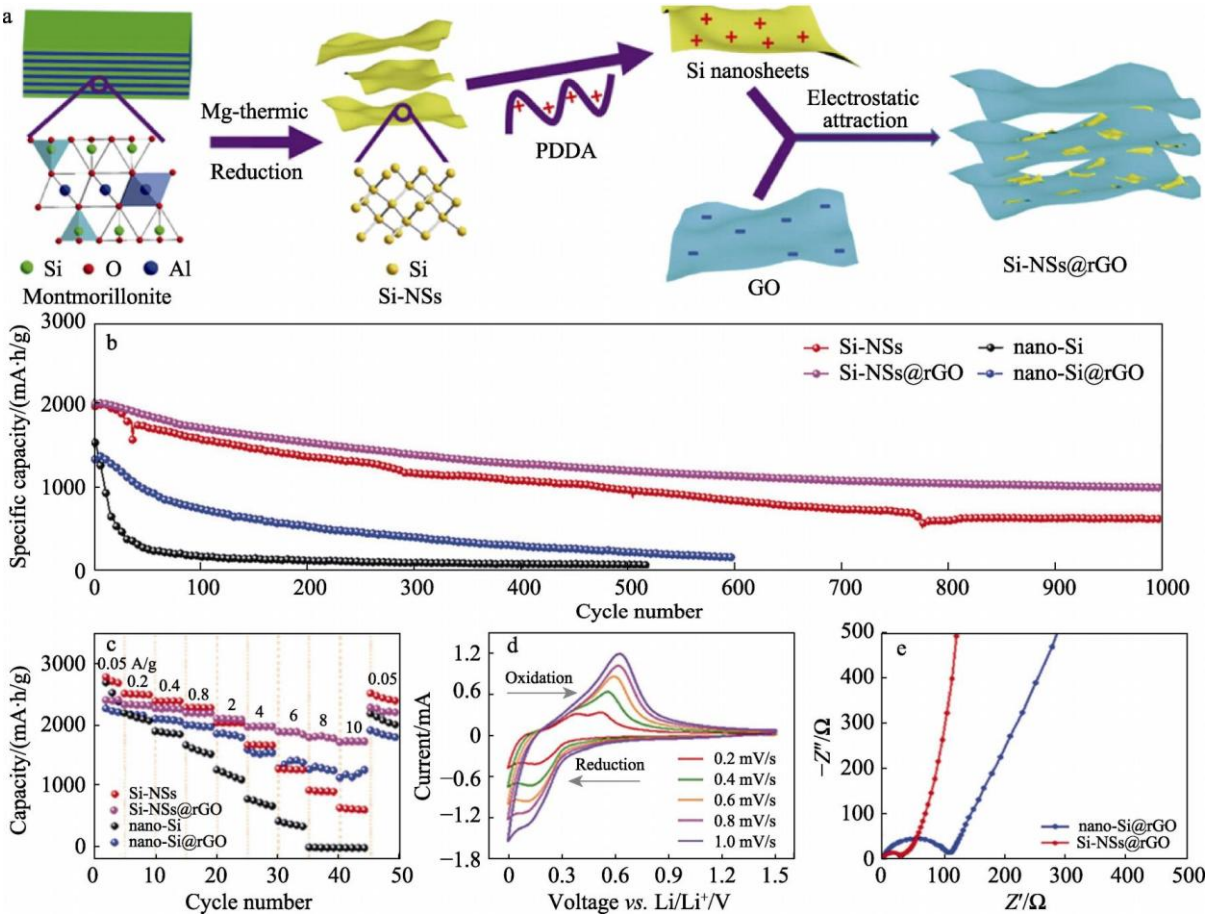

Figure 9 Schematic illustration of synthetic procedure for Si-NSs@rGO [75]

The realization of high-performance 2D silicon anodes is contingent upon the development of synthesis methodologies that balance structural precision, scalability, and cost-effectiveness. Vapor-phase techniques—primarily Chemical Vapor Deposition (CVD) and Physical Vapor Deposition (PVD)—remain the gold standard for producing atomically flat, defect-free silicon thin films. These methods offer exquisite control over thickness, crystallinity, and uniformity, making them indispensable for fundamental studies and thin-film battery architectures. However, the transition from laboratory-scale thin films to practical powder-based electrodes necessitates alternative routes capable of producing freestanding Si-NSs. Significant progress has been achieved through solution-based and solid-state reduction strategies. Qin et al. demonstrated a sophisticated multistep approach to fabricate 2D mesoporous silicon nanosheets encapsulated in carbon (pSi@C) via sol-gel templating, magnesiothermic reduction, and thermal decomposition. By employing cetyltrimethylammonium bromide-ethylenediaminetetraacetic acid (CTAB-EDTA) as a structure-directing agent, the researchers confined silicon growth within a 2D framework. The resulting composite leveraged synergistic advantages: the Si-NSs minimized vertical Li^+ diffusion distances, while the conformal carbon coating acted as a mechanical restraint to buffer volume expansion and stabilize the solid electrolyte interphase (SEI). This structural design yielded a reversible specific capacity of 2236.0 mAh/g after 150 cycles at 1 A/g and maintained 467.8 mAh/g after 500

cycles at 5 A/g, illustrating how rational template engineering bridges 2D structural advantages with practical cycling stability. Addressing scalability, Wei et al. developed a cost-effective magnesiothermic reduction strategy using low-cost bulk silicon powder as a precursor, eliminating the need for expensive silicon precursors. The resulting Si-NSs@C composite delivered a high reversible capacity of 2770 mAh/g at 0.1 C, an initial Coulombic efficiency of 87.9%, and a minimal capacity decay of 0.3% per cycle over 100 cycles at 0.5 C, underscoring the commercial viability of this route.

Despite these advances, 2D Si-based anodes face persistent challenges that must be addressed for commercial viability. The primary obstacle is the propensity of nanosheets to restack during slurry casting or cycling, which reduces accessible surface area, blocks ion channels, and negates the benefits of low dimensionality. Additionally, the synthesis of pristine silicene requires ultra-high vacuum epitaxial growth, rendering it prohibitively expensive for practical applications, while exfoliation methods often suffer from limited yield. To overcome these limitations, the field has evolved through several strategic iterations. Initial efforts focused on optimizing amorphous silicon layer thickness; more recent innovations emphasize coupling silicon with other elements (e.g., magnesium in magnesiothermic reduction) and integrating silicon into stabilizing active matrices such as magnesium silicate. The evolution of preparation methods—from early electrodeposition to modern magnetron sputtering and catalytic pyrolysis—reflects the maturation of thin-film technology and enhances the versatility of 2D silicon anodes. When benchmarked against traditional graphite, LIBs incorporating 2D silicon exhibit higher average output voltages, reduced electrode mass, and significantly extended cycle life. The 2D film structure optimizes the surface-area-to-volume ratio, shortens electron transfer distances, and suppresses polarization, while the planar geometry skillfully controls mechanical stress vectors by distributing strain laterally. Moving forward, the future success of 2D Si anodes lies in the continued refinement of structural design, where the unique properties of silicon are seamlessly integrated with synergistic materials to create robust, high-performance energy storage systems capable of meeting the demands of electric mobility and grid-scale storage.

3.4 3D Si-based Anode Materials

Three-dimensional (3D) macroporous silicon-based anode materials, encompassing porous silicon architectures and silicon nanosponges, represent the most structurally sophisticated strategy for reconciling the extreme volume expansion of silicon with the mechanical and kinetic demands of high-energy-density lithium-ion batteries (LIBs). Unlike lower-dimensional counterparts, 3D architectures leverage hierarchical porosity spanning nano- to macroscales to create a self-buffering system. The defining advantage of this design lies in its ability to decouple active material loading from structural integrity. Micropores and mesopores within the silicon framework provide dedicated reservoirs to accommodate the 300–400% volumetric expansion during lithiation, preventing catastrophic fracture and preserving electrical connectivity. Simultaneously, the continuous, interconnected network of electrode materials ensures efficient electron transport across the entire electrode thickness, mitigating the intrinsic insulating nature of silicon. Macropores, often exceeding hundreds of nanometers in diameter, serve as high-speed highways for liquid-phase Li^+ transport, drastically reducing diffusion overpotentials and polarization, particularly at high current densities. This multiscale porosity transforms the electrode from a rigid, brittle solid into a resilient, sponge-like structure capable of breathing during cycling. The result is a fundamental shift in failure mechanics: instead of particle pulverization and loss of contact, the electrode undergoes reversible elastic deformation, maintaining both capacity and structural cohesion over thousands of cycles. This architectural paradigm has become the gold standard for pushing silicon anodes toward commercial viability.

Despite their structural elegance, 3D macroporous silicon anodes face formidable challenges that must be overcome before widespread commercial adoption. Chief among these is the complexity and cost of fabrication. Methods such as electrochemical corrosion, templating, and 3D printing require precise control over pore uniformity and often involve multiple processing steps, increasing capital expenditure and process time. A more critical electrochemical limitation is the low first-cycle Coulombic efficiency (CE), typically around 70%, compared to >90% for commercial graphite. This deficit arises from the extensive surface area of 3D architectures, which promotes excessive solid electrolyte interphase (SEI) formation and irreversible lithium consumption. While subsequent cycles may achieve high efficiency, the initial lithium loss must be compensated via pre-lithiation strategies, adding manufacturing complexity. Furthermore, long-term cycling can induce pore collapse or

disconnection of the conductive network, accelerating capacity fade. The key technologies used in preparing 3D silicon anodes—magnesiothermic reduction, electrochemical displacement, and CVD—are inherently complex, demanding tight control over morphology and stoichiometry. Nevertheless, when benchmarked against 0D, 1D, and 2D designs, 3D nano-silicon currently represents the most promising technical route because it uniquely balances electrochemical performance with industrialization feasibility. Commercial lithium-ion batteries must simultaneously satisfy high power, high safety, low cost, long cycle life, and environmental sustainability. Table 2 summarizes the scalability potential and commercial prospects of advanced nano-silicon anodes across all dimensions. Ultimately, the successful translation of 3D silicon anodes will depend on simplifying synthesis, improving first-cycle efficiency, and demonstrating long-term stability in full-cell configurations with high-loading cathodes—milestones that will define the next decade of silicon battery research.

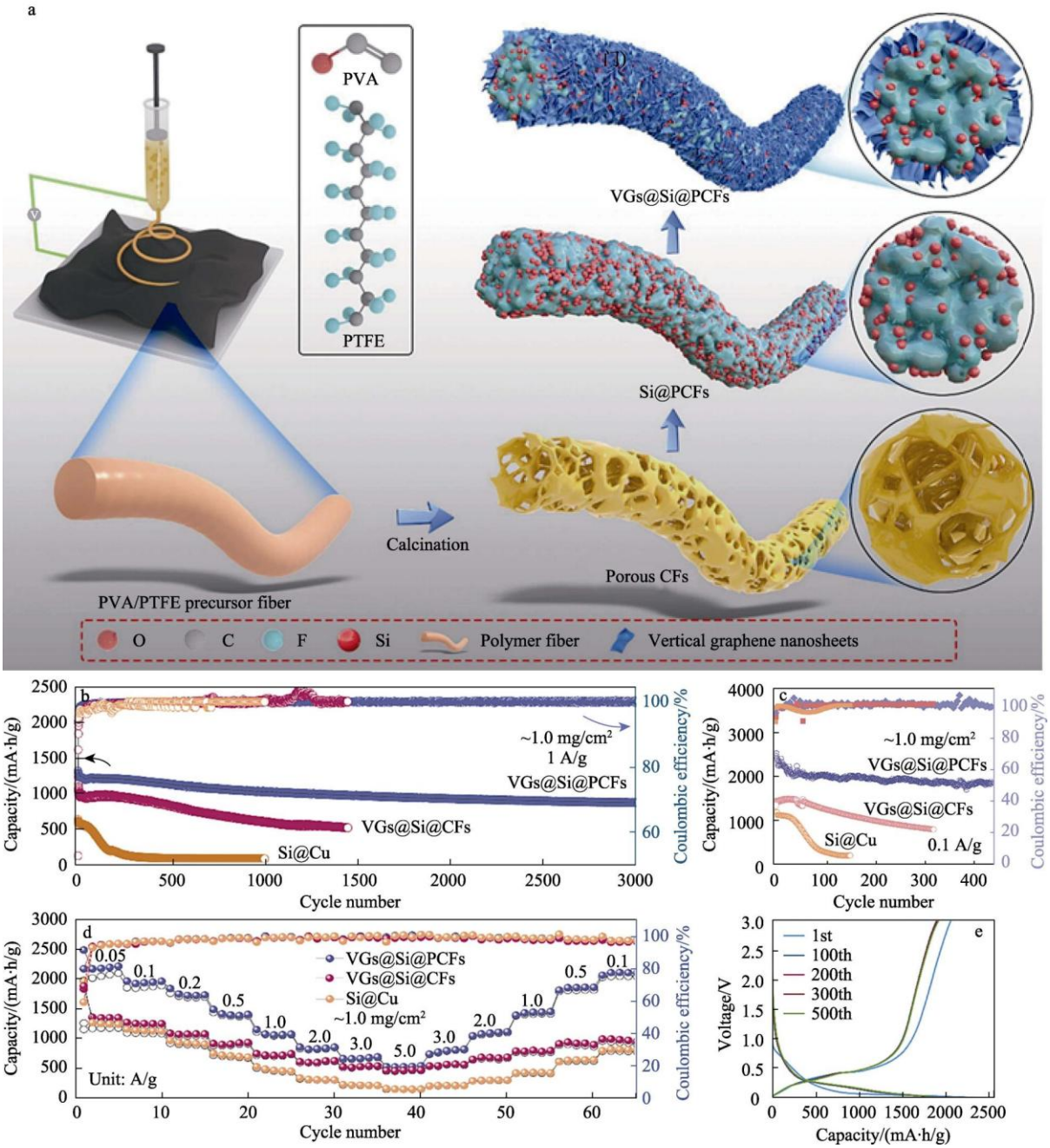

Figure 10 Schematic illustration for synthesis of VGs@Si@PCFs composite anode via electrospinning, magnetron sputtering and chemical vapor deposition method [60]

4 Discussion

4.1 hermodynamic and Kinetic Foundations of Silicon Anode Degradation, and the Rationale for Nanostructure-Mediated Stress Relaxation

The failure mechanisms of silicon-based anodes cannot be reduced to a simple narrative of “large volume expansion”; rather, they emerge from a tightly coupled set of thermodynamic instabilities, kinetic bottlenecks, and interfacial feedback loops that collectively destabilize the electrode across multiple length scales. At the atomic scale, the alloying reaction between silicon and lithium is governed by a free-energy landscape that favors the formation of increasingly lithiated amorphous phases, culminating in $Li_{15}Si_4$ or $Li_{4.4}Si$ at full lithiation. This transformation is accompanied by a 300–400% volumetric expansion, which is not isotropic but crystallographically biased, as revealed by the ledge-mechanism studies of Liu et al., where lithiation propagates via the sequential peeling of {111} planes and advances preferentially along <110> and <112> directions. Such anisotropic expansion generates localized compressive stresses that exceed the fracture toughness of crystalline silicon, leading to crack initiation on {100} planes and eventual particle pulverization. In amorphous silicon, while crystallographic anisotropy is absent, the absence of grain boundaries does not eliminate mechanical failure; instead, the homogeneous expansion induces global tensile stresses that still surpass the yield strength of the material under constrained electrode conditions. Compounding this mechanical instability is the chemical instability of the solid electrolyte interphase (SEI), which is not a static passivation layer but a dynamically evolving bilayer structure. During lithiation-induced expansion, the outer SEI layer experiences tensile strain that exceeds its cohesive limit, resulting in fracture and exposing fresh silicon surfaces to continuous electrolyte decomposition. This regenerative SEI growth consumes active lithium and electrolyte, thickens the interfacial resistance, and ultimately isolates active silicon domains from the electron-conductive network. The temperature dependence of these processes further complicates the picture: at elevated temperatures, lithiation proceeds via discrete crystalline intermediates ($Li_{12}Si_7$, $Li_{14}Si_6$, $Li_{13}Si_4$, $Li_{22}Si_5$), whereas at room temperature the reaction remains amorphous and kinetically sluggish, exacerbating polarization and irreversible capacity loss. Against this backdrop, nanostructure design emerges not merely as a performance enhancer but as a thermodynamic necessity. By reducing silicon dimensions to the nanoscale, the characteristic diffusion timescale (τ_D) becomes shorter than the reaction timescale (τ_R), shifting the rate-determining step from ion transport to interface propagation and enabling more uniform lithiation. Moreover, nanoscale architectures introduce free surfaces and internal voids that act as mechanical buffers, accommodating volumetric strain without generating catastrophic fracture. Zero-dimensional nanoparticles exemplify this principle: their high surface-to-volume ratio minimizes diffusion lengths, while internal porosity or yolk-shell designs provides dedicated expansion reservoirs. However, even nanostructuring cannot fully decouple mechanical and chemical degradation unless the interface between silicon and its surrounding matrix is rationally engineered. Carbon coatings, for instance, must balance rigidity and flexibility: overly rigid carbon shells suppress expansion but fracture, while overly flexible coatings fail to constrain particle motion and stabilize the SEI. Similarly, doping strategies—whether with nitrogen, sulfur, or transition metals—must enhance electronic conductivity without introducing new interfaces prone to side reactions. The implication is clear: nanostructure design must be accompanied by interfacial and compositional engineering to break the feedback loop between mechanical fracture and SEI regeneration. Without such holistic design, even the most elegantly architected silicon nanomaterials will remain confined to laboratory demonstrations rather than achieving commercial viability.

4.2 Multidimensional Nanostructure Performance Trade-Offs, Manufacturing Scalability, and the Roadmap Toward Commercial High-Energy-Density Anodes

The multidimensional nanostructure taxonomy presented in this review—spanning 0D nanoparticles and quantum dots, 1D nanowires and nanotubes, 2D nanosheets and silicene, and 3D porous sponges—reveals a rich design space but also exposes unavoidable performance trade-offs that must be navigated for real-world deployment. Zero-dimensional architectures, particularly silicon nanoparticles embedded in carbon matrices, offer the most straightforward route to high cycling stability and industrial compatibility. Their spherical symmetry distributes stress evenly, and when paired with nitrogen- or sulfur-doped carbon shells, they achieve Coulombic efficiencies above 99% and cycle lives exceeding 1000 cycles. However, their tap density is inherently low, leading to reduced volumetric energy density—a critical limitation for electric vehicle applications where space is constrained. One-dimensional structures, such as silicon nanowires and nanotubes, address this issue

by aligning electron and ion transport pathways along the axial direction, reducing tortuosity and improving rate capability. Their radial expansion mode is mechanically favorable, as it allows the structure to breathe without fracturing. Yet, the fabrication of 1D silicon anodes at scale remains challenging: metal-assisted chemical etching (MACE) and chemical vapor deposition (CVD) offer precise control but rely on expensive catalysts, hazardous reagents like HF, and energy-intensive processes incompatible with low-cost battery manufacturing. Two-dimensional silicon nanosheets and silicene push the limits of surface-dominated electrochemistry, offering ultrafast charge transfer and maximal exposure to the electrolyte. However, their structural fragility and tendency to restack during cycling severely limit practical implementation. Three-dimensional porous architectures, such as silicon nanosponges and inverse opals, represent perhaps the most promising compromise: they combine high active material loading with internal void space for expansion and continuous conductive frameworks. Nevertheless, their synthesis often involves templating routes that are difficult to scale and prone to structural collapse under high areal loading. Beyond geometry, the choice of preparation method introduces another layer of trade-offs. Mechanical ball milling is industrially mature and cost-effective but produces wide particle size distributions and introduces metallic impurities. Sol-gel and pyrolysis routes yield high-purity materials with controlled porosity but suffer from low throughput and high energy consumption. Template-based methods allow precise architectural control but are incompatible with continuous manufacturing lines. These limitations explain why, despite decades of academic progress, silicon anodes remain largely confined to niche applications or low-silicon-content blends with graphite. To bridge this gap, future research must prioritize scalable, dry-processing-compatible nanostructure fabrication, such as plasma-assisted synthesis or roll-to-roll vapor deposition. Equally important is the integration of silicon anodes with advanced electrolytes that stabilize the SEI through fluorinated solvents or film-forming additives, reducing the burden on nanostructure design alone. Full-cell validation under realistic conditions—high areal loading (>3 mAh/cm²), lean electrolyte, and extended cycling—must become the benchmark for new architectures, replacing half-cell metrics that often overestimate performance. Finally, economic and environmental life-cycle analyses should guide material selection, favoring earth-abundant dopants and recyclable carbon sources over exotic or toxic components. If these challenges are addressed in a coordinated fashion, multidimensional nano-silicon anodes could realistically deliver the 400–500 Wh/kg lithium-ion cells required for next-generation electric mobility, transforming silicon from a promising laboratory material into a commercial cornerstone of the energy transition.

4.3 Interface Chemistry, Electrolyte Co-Design, and the Systemic Integration of Silicon Anodes into Next-Generation Battery Platforms

While nanostructure engineering addresses the mechanical dimension of silicon anode failure, it does not operate in isolation; the electrochemical performance of silicon is equally dictated by the dynamic interplay between the active material, the solid electrolyte interphase, and the electrolyte formulation itself. The SEI layer, often described as a passive protector, is in reality a reactive, stress-sensitive membrane whose composition and mechanical properties determine whether a silicon anode survives hundreds or thousands of cycles. In conventional carbonate electrolytes, the SEI is rich in organic lithium alkyl carbonates, which are mechanically weak and prone to fracture under silicon's breathing motion. This triggers continuous electrolyte decomposition and lithium consumption, explaining the steep early-cycle capacity fade observed in unprotected silicon anodes. Recent advances in electrolyte engineering—such as the use of fluoroethylene carbonate (FEC), vinylene carbonate (VC), and lithium difluoro(oxalato)borate (LiDFOB)—have demonstrated that SEI chemistry can be tuned to form more inorganic-rich, mechanically robust interphases dominated by LiF and Li_2O. These species exhibit higher shear moduli and better adhesion to silicon surfaces, effectively decoupling SEI fracture from volume expansion. However, even the best electrolyte systems cannot fully compensate for poorly designed nanostructures: if the silicon particles are too large or lack internal void space, the strain energy released during lithiation will overwhelm any SEI, regardless of its composition. This interdependence underscores the need for co-design strategies, where nanostructure geometry, surface functionalization, and electrolyte formulation are optimized in parallel rather than sequentially. Another emerging frontier is the integration of silicon anodes with high-capacity cathodes, such as nickel-rich layered oxides (NCM, NCA) or sulfur cathodes, to realize full cells with energy densities exceeding 400 Wh/kg. These systems impose additional constraints: silicon's low working potential (~0.4 V vs. Li/Li^+) demands careful balancing to avoid lithium plating, while the high voltage of nickel-rich cathodes accelerates electrolyte oxidation and transition-metal dissolution, which can poison the SEI on the anode side. Pre-lithiation techniques—whether via lithium metal contact, stabilized lithium metal powder, or lithium silicate glass—have become essential to offset the irreversible lithium loss associated with SEI

formation, but they introduce safety and scalability concerns. Looking further ahead, the convergence of silicon anodes with solid-state electrolytes offers a potential breakthrough: solid polymer or sulfide electrolytes can mechanically suppress silicon expansion while eliminating flammable liquid components. However, interfacial resistance at the silicon–solid electrolyte boundary remains a major hurdle, requiring novel buffer layers or in-situ interface formation strategies. Life-cycle assessment also becomes critical at this stage, as the environmental footprint of silicon anode production—particularly energy-intensive CVD or magnesiothermic reduction—must be justified by the net reduction in battery-related CO_2 emissions over the vehicle lifetime. Recycling, too, must be rethought: silicon anodes complicate conventional hydrometallurgical recovery flows, necessitating new processes to reclaim both silicon and carbon fractions. Ultimately, the successful commercialization of multidimensional nano-silicon anodes will depend not on any single innovation but on the systemic integration of materials science, electrochemical engineering, manufacturing scalability, and sustainability metrics. The path forward is neither purely scientific nor purely engineering—it is a multidisciplinary endeavor where failure mechanisms, nanostructure design, and cell-level integration must be solved in concert.

5 Conclusion and Outlook

This paper outlines the reasons for the poor cycle stability of LIBs, and elaborates the latest progress in Si nanostructure design, and improves battery performance by optimizing the nanostructure of Si-based anodes. This comprehensive exploration marks the progress of Si-based anodes in multiple aspects, and emphasizes the importance of structural engineering in alleviating material stress challenges and improving the overall performance of batteries. With the continuous upgrading of high-efficiency energy storage systems in the future, Si-based anodes will play an increasingly important role in LIBs. To this end, several possible paths need to be explored and developed in the future:

(1) Adopt more innovative technologies to design nanostructures and optimize the preparation conditions of Si-based anode materials. Explore finer and more ingenious structures to further improve the cycle performance and life of LIBs. In addition, practical issues such as cost, process compatibility, and electrode engineering need to be considered to advance the commercialization of Si-based anodes.

(2) To improve the initial Coulombic efficiency and cycle performance of materials, materials with high conductivity can be selected for compounding in the future, or the particle morphology, microstructure, and chemical composition of materials can be adjusted by designing nanostructure engineering. To realize large-scale production and avoid resource waste on blind experiments, more research on the basic mechanism of materials and in-situ characterization needs to be carried out in the future. Some commonly used in-situ characterizations, such as SEM, TEM, and XRD, may help to evaluate various chemical reactions on the surface of Si-based materials. Combined with complex analysis techniques, such as in-situ FTIR, AFM, and NMR, as well as calculation methods, the connection between battery capacity and material structure at the atomic or molecular level can be better clarified, providing a better development prospect for the design of subsequent material structures.

(3) To improve the performance of LIBs, future research on Si-based anode materials can focus on the synergistic modification of the following points: develop more nanostructured Si-based materials, such as core-shell, yolk-shell, porous, and embedded structures; explore element doping, compounding of Si, and alloying strategies of Si with metal materials, metal oxides, and carbon-based materials; focus on surface modification of materials, such as artificial SEI film, surface coating, and surface functionalization; further strengthen the exploration of pre-lithiation technology for Si-based anodes.

(4) In addition to solving the unique challenges of LIBs Si-based anodes, it is equally important to develop suitable components for the entire battery system, including exploring suitable electrolytes, binders, separators, and cathode materials that work synergistically with Si-based anodes to improve the overall electrochemical performance of LIBs.

References

[1] Chen X B, Lu L, Yu P Y, et al. Increasing solar absorption for photocatalysis with black hydrogenated titanium dioxide nanocrystals. Science, 2011, 331(6018): 746-750.
[2] Li N, Zhang W, Li G X, et al. Research progress on TiO_2 photocatalysts. Fine Chemicals, 2021, 38(11): 2181-2188, 2258.
[3] Fuentes K M, Venuti D, Betancourt P. Black titania with increased defective sites for phenol photodegradation under visible light. Reaction Kinetics, Mechanisms and Catalysis, 2020, 131(1): 423-435.
[4] Andronic L, Lelis M, Enesca A, et al. Photocatalytic activity of defective black-titanium oxide photocatalysts towards pesticide degradation under UV/Vis irradiation. Surfaces and Interfaces, 2022, 32: 102123.
[5] Khanam R, Taparia D, Momdal B, et al. Black titania: Effect of hydrogenation on structural and thermal stability of nanotitania. Applied Physics A, 2016, 122(2): 92.
[6] Thakur N, Thakur N, Kumar A, et al. A critical review on the recent trends of photocatalytic, antibacterial, antioxidant and nanohybrid applications of anatase and rutile TiO_2 nanoparticles. Science of the Total Environment, 2020, 914: 169815.
[7] Haidner S, Nawaz R, Anjum M, et al. Property-performance relationship of core-shell structured black TiO_2 photocatalyst for environmental remediation. Frontiers of Environmental Science & Engineering, 2019, 17(9): 111.
[8] Soria J, Sanz J, Torralvo M J, et al. The effect of the surface disordered layer on the photoreactivity of titania nanoparticles. Applied Catalysis B: Environmental, 2017, 210: 306-319.
[9] Li Z, Wang E G, Zhang Y Z, et al. Antibacterial ability of black titania in dark: Via oxygen vacancies mediated electron transfer. Nano Today, 2019, 50: 101826.
[10] Jiang W B, Loh H Y, Low B Q L, et al. Role of oxygen vacancy in metal oxides for photocatalytic CO_2 reduction. Applied Catalysis B: Environmental, 2019, 321: 122079.
[11] Deskins N A, Du J, Rao P. The structural and electronic properties of reduced amorphous titania. Physical Chemistry Chemical Physics, 2017, 19(28): 18671-18684.
[12] Liu X G, Bi Y P. Synergistic effect of Ti^{3+} doping and facet regulation over Ti^{3+}-doped TiO_2 nanosheets with enhanced photoreactivity. Catalysis Science & Technology, 2018, 8(15): 3876-3882.
[13] Abdullah S A, Sahdan M Z, Nafarizal N, et al. Influence of substrate annealing on inducing Ti^{3+} and oxygen vacancy in TiO_2 thin films deposited via RF magnetron sputtering. Applied Surface Science, 2018, 462: 575-582.
[14] Gao X T. Study on photocatalytic properties based on TiO_{2-x} and its composites [D]. Harbin: Harbin Normal University, 2022.
[15] He M, Ji J, Liu B Y, et al. Reduced TiO_2 with tunable oxygen vacancies for catalytic oxidation of formaldehyde at room temperature. Applied Surface Science, 2019, 473: 934-942.
[16] Chen J, Ding Z Y, Wang C, et al. Black anatase titania with ultrafast sodium-storage performances stimulated by oxygen vacancies. ACS Applied Materials & Interfaces, 2016, 8(14): 9142-9151.
[17] Shi D X, Zhang H H, Gao X, et al. Research progress on the preparation and catalytic application of core-shell nanocomposites. Fine Chemicals, 2019, 40(1): 33-43.
[18] Hu W Y, Zhou W, Zhang K F, et al. Facile strategy for controllable synthesis of stable mesoporous black TiO_2 hollow spheres with efficient solar-driven photocatalytic hydrogen evolution. Journal of Materials Chemistry A, 2016, 4(19): 7495-7502.
[19] Zhang K, Park J H. Surface localization of defects in black TiO_2: Enhancing photoactivity or reactivity. The Journal of Physical Chemistry Letters, 2017, 8(1): 199-207.
[20] Zhang S S, Zhang S Q, Peng B Y, et al. High performance hydrogenated TiO_2 nanorod arrays as a photoelectrochemical sensor for organic compounds under visible light. Electrochemistry Communications, 2014, 40: 24-27.
[21] Wang Z, Yang C Y, Lin T, et al. H-doped black titania with very high solar absorption and excellent photocatalysis enhanced by localized surface plasmon resonance. Advanced Functional Materials, 2013, 23(43): 5444-5450.
[22] Pylnev M, Chang W H, Wong M S. Shell of black titania prepared by sputtering TiO_2 target in H_2+Ar plasma. Applied Surface Science, 2018, 462: 285-290.
[23] Ariyanti D, Mills L, Dong J, et al. $NaBH_4$ modified TiO_2: Defect site enhancement related to its photocatalytic activity. Materials Chemistry and Physics, 2017, 199: 571-576.
[24] Chen S H, Xiao Y, Wang Y H, et al. A facile approach to prepare black TiO_2 with oxygen vacancy for enhancing photocatalytic activity. Nanomaterials, 2018, 8(4): 245.
[25] Zheng P, Tang J L, Zhou Z P, et al. Ultrafast synthesis of defective black TiO_2 via one-step NaN_3 deflagration

for high-efficiency solar water evaporation. Surfaces and Interfaces, 2020, 22: 100901.
[26] Wang Z, Yang C Y, Lin T Q, et al. Visible-light photocatalytic, solar thermal and photoelectrochemical properties of aluminium-reduced black titania.Energy & Environmental Science, 2013, 6(10): 3007-3014.
[27] Lin L X, Huang J T, Li X F, et al. Effective surface disorder engineering of metal oxide nanocrystals for improved photocatalysis. Applied Catalysis B: Environmental, 2017, 203: 615-624.
[28] Azab N A, El-Sharkawy A A M, Omran Z A, et al. C_3N_4 interlayer formation while synthesizing black titania and their dye sensitized solar cell and conductivity performances. Solar Energy Materials and Solar Cells, 2021, 232: 111347.
[29] Qi W T, Wang N, Chen X Y, et al. Plasmon-assisted partially reduced TiO_2 nanotube arrays for photoelectrochemical water splitting. Materials Research Express, 2020, 6(12): 1250h9.
[30] Li Z B, Bian H D, Xiao X F, et al. Defective black TiO_2 nanotube arrays for enhanced photocatalytic and photoelectrochemical applications. ACS Applied Nano Materials, 2019, 2(11): 7372-7378.
[31] Liu X, Xu H, Grabstanowicz L R, et al. Ti^{3+} self-doped TiO_{2-x} anatase nanoparticles via oxidation of TiH_2 in H_2O_2. Catalysis Today, 2014, 225: 80-89.
[32] Reddy Y A K, Kang I K, Shin Y B, et al. Oxygen atmosphere annealing effect on the thermal stability of TiO_{2-x} based films for shutter-less infrared image sensors. Key Engineering Materials, 2018, 775: 272-277.
[33] Su Y, Zhang W, Chen S M, et al. Engineering black titanium dioxide by femtosecond laser filament. Applied Surface Science, 2020, 520: 146298.
[34] Jedsukontorn T, Ueno T, Saito N, et al. Facile preparation of defective black TiO_2 through the solution plasma process: Effect of parametric changes for plasma discharge on its structural and optical properties. Journal of Alloys and Compounds, 2017, 726: 567-577.
[35] Raes A, Ninakanti R, Van den B L, et al. Black titania by sonochemistry: A critical evaluation of existing methods. Ultrasonics Sonochemistry, 2019, 100: 106601.
[36] Zhang L N, Liu T L, Liu T F, et al. Improving photocatalytic performance of defective titania for carbon dioxide photoreduction by Cu cocatalyst with SCN^- ion modification. Chemical Engineering Journal, 2019, 463: 142358.
[37] Bi Q Y, Song E, Chen J C, et al. Nano gold coupled black titania composites with enhanced surface plasma properties for efficient photocatalytic alkyne reduction. Applied Catalysis B: Environmental, 2022, 309: 121222.
[38] Cong T Z, Zhang Y F, Huang H, et al. Ag nanoparticles synthesized on black-titanium dioxide by photocatalytic method as reusable substrates of surface-enhanced Raman spectroscopy. Chemosensors, 2022, 10(11): 441.
[39] Yuan C F, Shen Y L, Zhu C Y, et al. Ru single-atom decorated black TiO_2 nanosheets for efficient solar-driven hydrogen production. ACS Sustainable Chemistry & Engineering, 2022, 10(31): 10311-10317.
[40] Yuan X T, Wang X, Liu X Y, et al. Ti^{3+}-promoted high oxygen-reduction activity of Pd nanodots supported by black titania nanobelts. ACS Applied Materials & Interfaces, 2016, 8(41): 27654-27660.
[41] Yang C Y, Wang Z, Lin T Q, et al. Core-shell nanostructured "black" rutile titania as excellent catalyst for hydrogen production enhanced by sulfur doping. Journal of the American Chemical Society, 2013, 135(47): 17831-17838.
[42] Rahman S, Nawaz R, Khan J, et al. Synthesis and characterization of carbon and carbon-nitrogen doped black TiO_2 nanomaterials and their application in sonophotocatalytic remediation of treated agro-industrial wastewater. Materials, 2021, 14(20): 6175.
[43] Shafiee A, Carrier A J, Nganou C, et al. Mechanistic insight into the enhanced photodegradation by black titanium dioxide nanofiber-graphene quantum dot composites. Applied Surface Science, 2019, 636: 157836.
[44] Cui H, Cao J Y, Zhao Y, et al. Construction of IO-B-TiO_2/In_2O_3 S-scheme heterojunction with photothermal effects and its highly efficient photocatalytic reduction of CO_2 under full-spectrum light. Chemical Engineering Journal, 2020, 479: 147618.
[45] Li Y F, Feng Y C, Bai H, et al. Enhanced visible-light photocatalytic performance of black TiO_2/SnO_2 nanoparticles. Journal of Alloys and Compounds, 2019, 960: 170672.
[46] Li Z Z, Li H Z, Wang S J, et al. Mesoporous black TiO_2/MoS_2/Cu_2S hierarchical tandem heterojunctions toward optimized photothermal-photocatalytic fuel production. Chemical Engineering Journal, 2022, 427: 131830.
[47] Tan B Y, Ye X Z, Li Y J, et al. Defective anatase TiO_{2-x} mesocrystal growth in situ on g-C_3N_4 nanosheets: Construction of 3D/2D Z-scheme heterostructures for highly efficient visible-light photocatalysis. Chemistry—A European Journal, 2018, 24(50): 13311-13321.
[48] Li J, Jiang Z X, Li J F, et al. Synthesis of black titanium dioxide/activated carbon composites for enhanced visible-light photocatalytic properties. Journal of Materials Science: Materials in Electronics, 2020, 35(16):

1050.

[49] Zakaria H, Li Y, Fathy M M, et al. A novel TiO_{2-x}/TiN@ACB composite for synchronous photocatalytic Cr(VI) reduction and water photothermal evaporation under visible/infrared light illumination. Chemosphere, 2019, 311: 137137.

[50] Hu P W, Zhang Y, Cheng G L. Natural kaolinite modified black titanium dioxide for efficient visible light assisted photocatalysis. Molecular Catalysis, 2019, 547: 113312.

[51] Zhai M J, Liu Y, Huang J, et al. Efficient suspension plasma spray fabrication of black titanium dioxide coatings with visible light absorption performances. Ceramics International, 2019, 45(1): 930-935.

[52] Chen S H, Wang Y H, Li J, et al. Synthesis of black TiO_2 with efficient visible-light photocatalytic activity by ultraviolet light irradiation and low temperature annealing. Materials Research Bulletin, 2018, 98: 280-287.

[53] Saensook S, Sirisuk A. A factorial experimental design approach to obtain defect-rich black TiO_2 for photocatalytic dye degradation. Journal of Water Process Engineering, 2022, 45: 102495.

[54] Yuan X J, Sun M X, Yao Y, et al. N/Ti^{3+}-codoped triphasic TiO_2/g-C_3N_4 heterojunctions as visible-light photocatalysts for the degradation of organic contaminants. New Journal of Chemistry, 2019, 43(6): 2665-2675.

[55] Chen P. A novel synthesis of Ti^{3+} self-doped Ag_2O/TiO_2 (p-n) nanoheterojunctions for enhanced visible photocatalytic activity. Materials Letters, 2016, 163: 130-133.

[56] Wang S C, Cai J S, Mao J J, et al. Defective black Ti^{3+} self-doped TiO_2 and reduced graphene oxide composite nanoparticles for boosting visible-light driven photocatalytic and photoelectrochemical activity. Applied Surface Science, 2019, 467: 45-55.

[57] Jiang X D, Zhang Y P, Jiang J, et al. Characterization of oxygen vacancy associates within hydrogenated TiO_2: A positron annihilation study. The Journal of Physical Chemistry C, 2012, 116(42): 22619-22624.

[58] Pradenas M, Yanez J, Ranganathan S, et al. Multivariate approach to hydrogenated TiO_2 photocatalytic activity under visible light. Water Environment Research, 2019, 91(2): 157-164.

[59] An H R, Park S Y, Kim H, et al. Advanced nanoporous TiO_2 photocatalysts by hydrogen plasma for efficient solar-light photocatalytic application. Scientific Reports, 2016, 6(1): 29683.

[60] Wang X T, Li Y M, Liu X, et al. Preparation of Ti^{3+} self-doped TiO_2 nanoparticles and their visible light photocatalytic activity. Chinese Journal of Catalysis, 2015, 36(3): 389-399.

[61] Han L J, Su B T, Liu G, et al. A facile microwaving method to turn titanium oxide into highly active Ti^{3+} self-doped structure. Journal of Nanoscience and Nanotechnology, 2016, 16(9): 9826-9831.

[62] Li G L, Li J, Li G, et al. N and Ti^{3+} co-doped 3D anatase TiO_2 superstructures composed of ultrathin nanosheets with enhanced visible light photocatalytic activity. Journal of Materials Chemistry A, 2015, 3(44): 22073-22080.

[63] Zhang H, Xing Z P, Zhang Y, et al. Ni^{2+} and Ti^{3+} co-doped porous black anatase TiO_2 with unprecedented-high visible-light-driven photocatalytic degradation performance. RSC Advances, 2015, 5(129): 107150-107157.

[64] Du J M, Wang H M, Chen H J, et al. Synthesis and enhanced photocatalytic activity of black porous Zr-doped TiO_2 monoliths. Nano, 2016, 11(6): 1650068.

[65] Nawaz R, Kait C F, Chia H Y, et al. Glycerol-mediated facile synthesis of colored titania nanoparticles for visible light photodegradation of phenolic compounds. Nanomaterials, 2019, 9(11): 1586.

[66] Han K, Zhang X, Wang H F, et al. A facile microwaving method to turn titanium oxide into highly active Ti^{3+} self-doped structure. Journal of Nanoscience and Nanotechnology, 2016, 16(9): 9826-9831.

[67] Zhou G, Meng H Y, Cao Y, et al. Surface plasmon resonance-enhanced solar-driven photocatalytic performance from Ag nanoparticles-decorated Ti^{3+} self-doped porous black TiO_2 pillars. Journal of Industrial and Engineering Chemistry, 2018, 64: 188-193.

[68] Qiao P Z, Sun B J, Li H Z, et al. Surface plasmon resonance-enhanced visible-NIR-driven photocatalytic and photothermal catalytic performance by Ag/mesoporous black TiO_2 nanotube heterojunctions. Chemistry—An Asian Journal, 2019, 14(1): 177-186

[69] Bazzanella N, Bajpai O P, Fendrich M, et al. Ciprofloxacin degradation with a defective TiO_{2-x} nanomaterial under sunlight. MRS Communications, 2019, 13(6): 1252-1259.

[70] Feng X Y, Wang P F, Hou J, et al. Oxygen vacancies and phosphorus codoped black titania coated carbon nanotube composite photocatalyst with efficient photocatalytic performance for the degradation of acetaminophen under visible light irradiation. Chemical Engineering Journal, 2018, 352: 947-956.

[71] Wu S Q, Li X Y, Tian Y Q, et al. Excellent photocatalytic degradation of tetracycline over black anatase-TiO_2 under visible light. Chemical Engineering Journal, 2021, 406: 126747.

[72] Ren L P, Zhou W, Sun B J, et al. Defects-engineering of magnetic γ-Fe_2O_3 ultrathin nanosheets/mesoporous

black TiO_2 hollow sphere heterojunctions for efficient charge separation and the solar-driven photocatalytic mechanism of tetracycline degradation. Applied Catalysis B: Environmental, 2019, 240: 319-328.

[73] He J H, Ye J, Zhang Y, et al. Synergistic RGO/black TiO_2/2D-ZIF-8 ternary heterogeneous composite with highly efficient photocatalytic activity. ChemistrySelect, 2020, 5(12): 3746-3755.

[74] Cao Y, Xing Z P, Hu M Q, et al. Mesoporous black N-TiO_2-hollow spheres as efficient visible-light-driven photocatalysts. Journal of Catalysis, 2017, 356: 246-254.

[75] Yan Z Y, Huang W X, Jiang X R, et al. Hollow structured black TiO_2 with thickness-controllable microporous shells for enhanced visible-light-driven photocatalysis. Microporous and Mesoporous Materials, 2021, 323: 111228.

[76] Li G S, Lian Z C, Li X, et al. Ionothermal synthesis of black Ti^{3+}-doped single-crystal TiO_2 as an active photocatalyst for pollutant degradation and H_2 generation. Journal of Materials Chemistry A, 2015, 3(7): 3748-3756.